Quantum Mechanical Tunneling in the Unimolecular Dissociation of the Propargyl Bromide Molecular Ion

Doo Young Kim,[†] Joong Chul Choe,[‡] and Myung Soo Kim*,[†]

National Creative Research Initiative Center for Control of Reaction Dynamics and Department of Chemistry, Seoul National University, Seoul 151-742, Korea, and Department of Chemistry, University of Suwon, Suwon 440-600, Korea

Received: February 11, 1999; In Final Form: April 15, 1999

The Br loss of the propargyl bromide molecular ion has been studied using the mass-analyzed ion kinetic energy spectrometry. The kinetic energy release distribution in the unimolecular dissociation has been determined. The potential energy surface for the mechanistic pathway has been investigated by quantum chemical calculations on the B3LYP/6-311G** density functional theory level. Geometries and energies of five isomeric molecular ions, products, and related transition states have been determined. Calculation of the rate constants with statistical rate models predicts that the product $C_3H_3^+$ ion has only the cyclopropenium structure and that the observed unimolecular reaction occurs via tunneling through an isomerization barrier for the H-atom transfer.

1. Introduction

The potential energy surface (PES) provides invaluable information on dissociation dynamics of molecular systems.[1−14] Tremendous efforts have been made over the years to obtain PES through quantum chemical calculation, and the method is routinely applied to various systems, both neutrals[2,3] and ions.[4−14] PES thus constructed can be combined with classical trajectory[3−6] or statistical[7−11] calculations to interpret experimental observations such as rate constant, product energy distribution, and intramolecular energy transfer. Recent studies include investigation of the quantum mechanical tunneling effect in the dissociation dynamics of polyatomic ions.[8] For example, the tunneling correction[15] to the transition state theory calculation, which can be made by utilizing PES characteristics near the transition state, has been found to lead to better agreements between experimental and calculated rate constants.[8] This is especially important for a reaction involving H-atom transfer across a barrier.

Investigation of the exit channel behavior is as much important as the entrance channel study for a comprehensive understanding of dissociation dynamics.[16−21] Useful information on the former is available from the experimental and calculated product energy disposal data. In the case of ionic dissociation, the energy partitioned to the relative translation of products, namely the kinetic energy release (KER), or its distribution (KERD) can be readily measured by a variety of mass spectrometric methods[17,22−25] and provides an especially useful tool for the exit channel study. Rigorous theoretical studies[6] utilizing the classical trajectory method have been made to interpret the experimental KERD data. However, the KERD data have been more often utilized on the phenomenological level to gain some qualitative information on the dissociation process.[16−21] For example, the kinetic energy release, which is noticeably larger than statistically expected, is an indication of the presence of the reverse barrier in the exit channel. Also useful is the case when KERD appears as bimodal, which is an indication of the formation of isomeric products. Then, it is often possible to determine the branching ratio by analyzing this bimodal KERD.[19−21]

Experimental and theoretical studies have been carried out on the production of isomeric $C_3H_3^+$ ions from several molecular ions such as propargyl halides[26−31] and 1-butyne.[30] Of the two isomeric species generated, namely cyclopropenium ion (cyclo-$C_3H_3^+$, CP) and propargyl ion ($CH{\equiv}CCH_2^+$, PG), the former is known to be more stable than the latter by ~100 kJ mol^{-1}.[14,32] Dissociations of propargyl bromide and chloride molecular ions have been studied by several methods such as photoelectron−photoion coincidence (PEPICO),[26,27] photodissociation,[28] metastable ion decomposition (MID),[28−30] collision-induced dissociation (CID),[30] and ion cyclotron resonance[31] spectrometries. In the PEPICO study performed by Tsai et al.,[27] the rate constant for the dissociation of the propargyl bromide ion to $C_3H_3^+$ could not be determined because the rate constant was presumably larger than could be determined by the technique even at the reaction threshold (10^7 s^{-1} or larger). On the other hand, Holmes and co-workers[29,30] and Krailler and Russell[28] reported the observation of the unimolecular dissociation (MID) of the propargyl bromide ion with double focusing mass spectrometers. These instruments detect reactions occurring a few tens of microseconds after the formation of the molecular ions. Hence, it is surprising to note that the reaction with the rate constant larger than 10^7 s^{-1} even at the threshold was observable with such instruments.

In the present study, the Br loss of the propargyl bromide (3-bromo-1-propyne) molecular ion (PGB) has been reinvestigated.

$$CH{\equiv}CCH_2Br^{\bullet+} \rightarrow C_3H_3^+ + Br^{\bullet} \qquad (1)$$

The KERD in the unimolecular dissociation has been determined. Quantum chemical calculations have been carried out to probe the PES along which the reaction proceeds. The

* To whom correspondence should be addressed.
[†] Seoul National University.
[‡] University of Suwon.

10.1021/jp990526+ CCC: $18.00
Published on Web 05/27/1999

transition state theory rate constants have been calculated with the tunneling correction when needed to understand the occurrence of the reaction on a microsecond time scale.

2. Experimental Section

A double focusing mass spectrometer with reverse geometry (VG Analytical Model ZAB-E) was used for investigation. Samples were introduced into the ion source via a septum inlet and ionized by 70 eV electron ionization. The ion source temperature was maintained at 180 °C, and ions generated were accelerated to 8 keV. Mass-analyzed ion kinetic energy spectrometry (MIKES) was used to observe the MID or CID of molecular ions. Namely, the molecular ion was separated by the magnetic sector and the translational kinetic energy of a product ion generated in the second field-free region of the instrument was analyzed by the electric sector. To improve the analysis of an MID peak, the spectrum was acquired with the electrode assembly near the intermediate focal point of the instrument floated at a high voltage.[19] The peak for MID occurring inside the electrode assembly can be separated from that occurring outside in this way. Then, the time between the molecular ion formation and its unimolecular dissociation, namely, the lifetime of the metastable ion decomposition, is narrowly defined. This is 28 μs for $C_3H_3Br^{\bullet+}$ accelerated to 8 keV, which corresponds to 1.9×10^4 s^{-1} in rate constant. In a usual CID experiment, He gas was introduced into the collision cell located near the intermediate focal point such that the molecular ion beam is attenuated by 10%. To improve the quality of a MIKE spectrum, signal averaging was carried out for repetitive scans.

Propargyl bromide was the best grade commercially available. Bromoallene was prepared by treating propargyl bromide with triphenylphosphine in toluene according to the method of Jacobs and Brill.[33] The final product after a workup process contained toluene and diethylamine as well as bromoallene, while propargyl bromide was removed completely. The mixture was used without further purification to obtain a MIKE spectrum of MID or CID of bromoallene ion since the molecular ion (*m*/*z* 118) was not contaminated by ions from toluene or diethylamine.

3. Computational Section

Quantum chemical calculations were performed for various geometries related to the dissociation of PGB using the Gaussian 94[34] suite of programs on CRAY-T3E and IBM SP2 computers. These include five isomeric $C_3H_3Br^{\bullet+}$ ions and two $C_3H_3^+$ ions. Transition state (TS) geometries connecting these structures were searched. TS geometries found were checked by calculating the intrinsic reaction coordinates (IRCs). Calculations were attempted at the Hartree−Fock (HF), the second-order Møller−Plesset (MP2), and the B3LYP density functional levels of theory using the standard 6-311G** basis set. A complete identification of the reaction pathways could not be made at the HF and MP2 levels in the sense that some of the TS structures could not be found. In addition, the HF level calculation resulted in one imaginary frequency for the optimized PGB geometry. On the other hand, the MP2 level calculation suffered from serious spin contamination. The B3LYP calculations were free from these difficulties and will be presented here.

4. Results and Discussion

In the MID-MIKE spectrum of PGB obtained in this work, $C_3H_3^+$ was the only product ion. The MID-MIKE spectrum obtained with the electrode assembly floated at 2 kV is shown in Figure 1a. In the figure, only the MIKE profile of $C_3H_3^+$ generated inside the electrode assembly is shown. The peak, which looks dish-topped, was very weak. Referring to the PEPICO study[27] mentioned in a previous section, it is possible that the peak was generated not by unimolecular reaction (MID) but by CID due to the residual gas. To rule out such a possibility, the CID experiment was carried out. The $C_3H_3^+$ peak intensity increased by a factor of 60 as the He gas was introduced to the collision cell to the pressure resulting in 10% attenuation of the precursor ion beam. The change in the MIKE profile was even more spectacular. As the collision gas was introduced, a sharp peak appeared at the center of the dish and its intensity increased with the collision gas pressure. On the other hand, the intensity of the dished component, the peak shown in Figure 1a, was hardly affected by the collision gas pressure. This indicates that the peak in Figure 1a obtained without introducing the collision gas originates from the unimolecular dissociation (MID) of $C_3H_3Br^{\bullet+}$, not from CID. Burgers et al. reported the appearance of a weak Gaussian-type component at the center of the dish for the same reaction.[30] The present result shows that their observation was not free from the contamination by CID. The method to evaluate KERD from a MIKE profile was reported previously.[25] KERD for the reaction obtained by analyzing the MIKE profile in Figure 1a is shown in Figure 1b. The average value of KER evaluated from the distribution is 530 meV, which is in decent agreement with 477 meV reported by Krailler and Russell.[28]

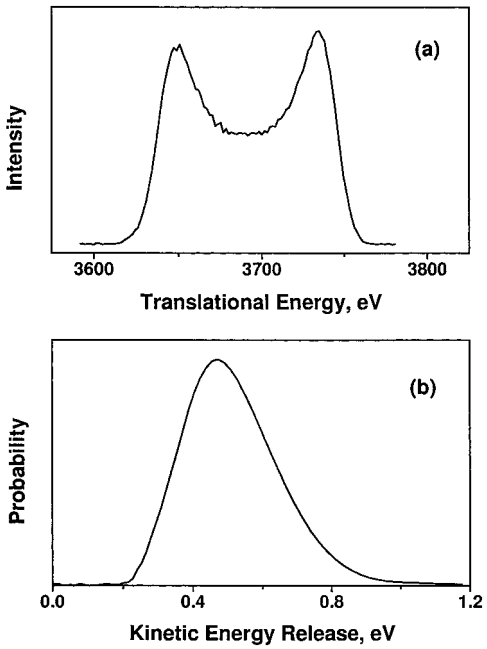

Figure 1. (a) MID-MIKE profile of $C_3H_3^+$ from $C_3H_3Br^{\bullet+}$ generated by electron ionization of the propargyl bromide neutral. The electrode assembly was floated at 2 keV. (b) Kinetic energy release distribution evaluated for the profile in (a).

It is well-known that the propargyl bromide ion (PGB) dissociates either to cyclopropenium (CP) or to propargyl (PG) ions.

$$\underset{\text{(PGB)}}{CH{\equiv}CCH_2Br^{\bullet+}} \rightarrow \begin{cases} \text{cyclo-}C_3H_3^+ + Br^{\bullet} \quad \text{(CP)} & (2a) \\ CH{\equiv}CCH_2^+ + Br^{\bullet} \quad \text{(PG)} & (2b) \end{cases}$$

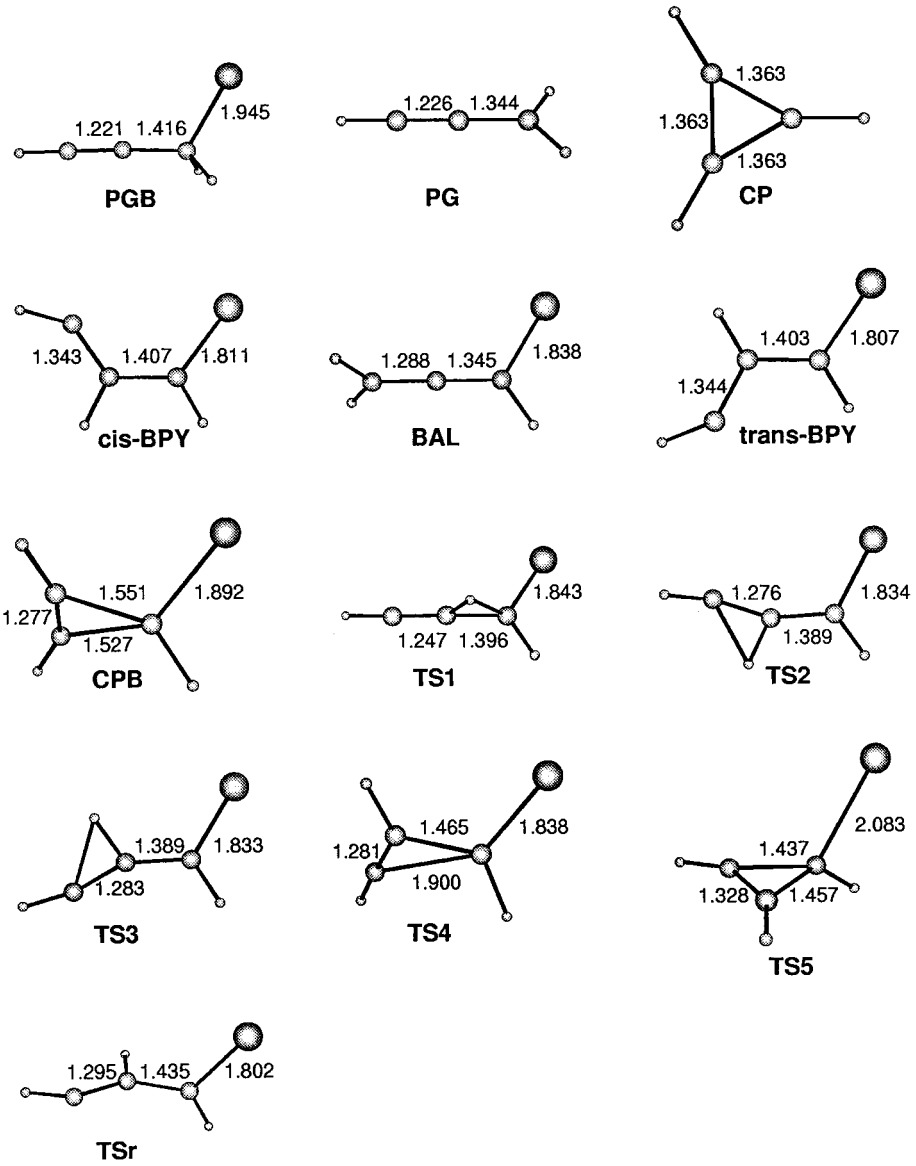

Figure 2. Structures of relevant chemical species determined by the quantum chemical calculations on the B3LYP/6-311G** density functional theory level. Numbers are the bond lengths in Å. PGB = propargyl bromide ion, PG = propargyl ion, CP = cyclopropenium ion, BAL = bromoallene ion, BPY = 1-bromo-1-propen-3-ylidene ion, CPB = cyclopropenyl bromide ion, TS1−TSr = transition state structures. (See Figure 3.)

It is likely that reaction 2b is a simple bond cleavage occurring with hardly any reverse barrier, as is confirmed by the quantum chemical calculation (see Figure 3). For such a reaction, it is well established that the statistical phase space theory provides a good description for its KERD.[17−20] Then, a relatively small fraction of the available energy is released into the translational degree of freedom and the maximum of the distribution appears near the zero energy release. The KERD in Figure 1b, which starts at 0.2 eV and extends up to 1 eV, does not fit the characteristics of a simple bond cleavage. Rather, its shape is typical for a dissociation occurring with a considerable reverse barrier. This led previous investigators to conclude that CP was the major product ion near the threshold.[28−30]

To summarize the observations made so far, we have found that the cyclopropenium ion (CP) is generated predominantly in the dissociation of the propargyl bromide molecular ion near the reaction threshold. This is in contrast with the previous PEPICO[27] and MID[30] studies where the production of the propargyl ion (PG) was also reported. Considering that the rate constant for the dissociation of PGB is larger than 10^7 s^{-1} at the threshold, as indicated by the PEPICO study, it is interesting to note that reaction 2a is observed even after the time delay of 28 μs in this experiment. We attempted to calculate the rate constants for reactions 2a and 2b with the Rice−Ramsperger−Kassel−Marcus (RRKM) theory using the critical energies of 0.52 eV, as indicated by the PEPICO study, and varying the entropy of activation over a wide range (−21 to +42 J mol^{-1} K^{-1}). The RRKM rate constants thus obtained were always larger than 10^8 s^{-1}, even at the threshold, in agreement with the PEPICO study. As an effort to find out the proper explanation for the above seemingly conflicting observations, we calculated the pertinent potential energy surface by the quantum chemical methods.

Quantum Chemical Calculations. Calculations at the B3LYP/6-311G** density functional theory level have shown that several isomerization steps are involved in reaction 2a. Intermediates and transition states appearing in the reaction channels that are plausible near the dissociation threshold have been found at this level of theory. Their structures are shown in Figure 2 together with those for PGB, PG, and CP ions. Both the potential energies and harmonic vibrational frequencies for these structures were calculated. The vibrational frequencies are listed in

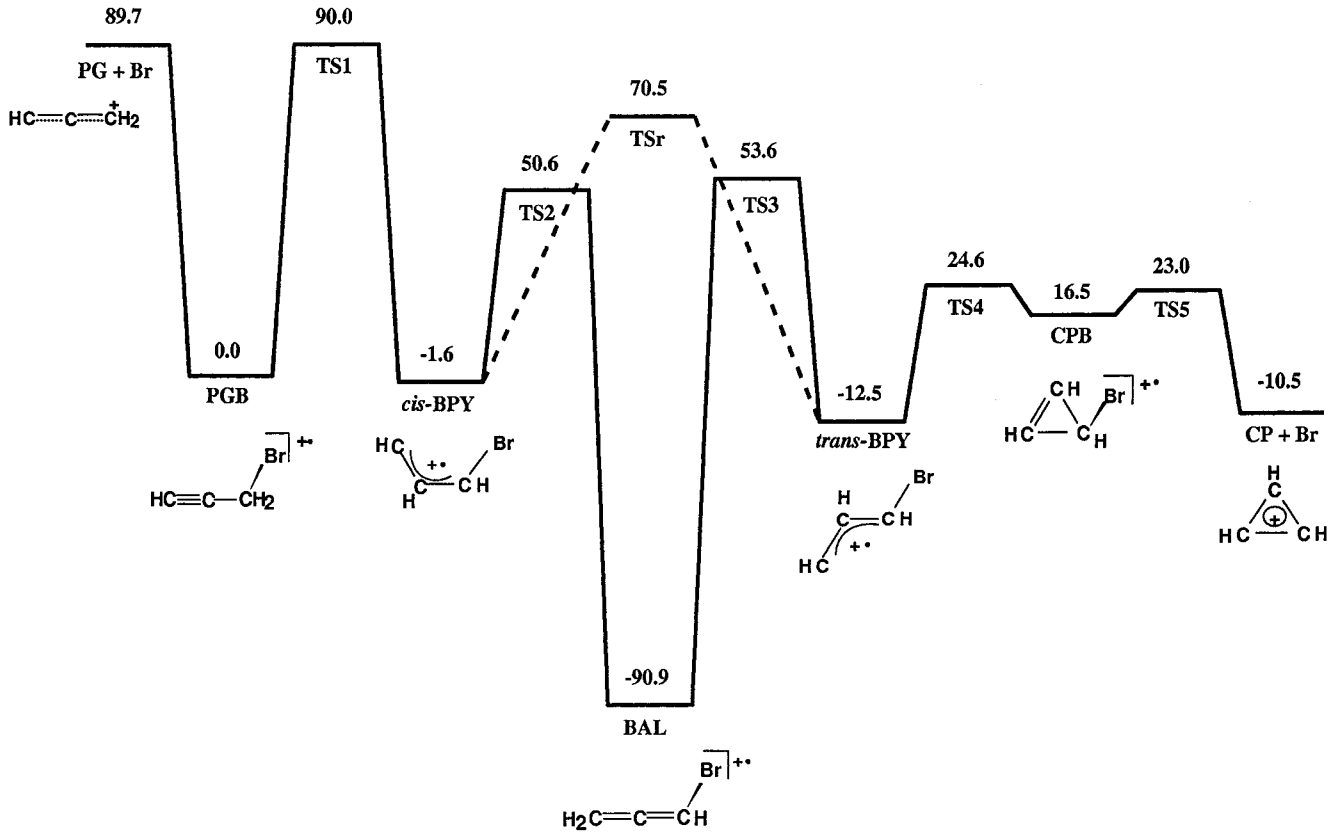

Figure 3. Potential energy surface calculated on the B3LYP/6-311G** density functional theory level. Numbers are the potential energies at the zero points referred to that of PGB. See the caption of Figure 2 for abbreviations.

TABLE 1: Potential Energies and Vibrational Frequencies of the Relevant Chemical Structures

species[a]	potential energies[b] (kJ mol^{-1})	vibrational frequencies (cm^{-1})
reactant		
PGB	0.00	164, 280, 397, 555, 621, 727, 738, 1007, 1060, 1129, 1291, 2109, 2935, 2948, 3401
products		
CP[c]	−10.47	775, 936, 936, 1020, 1020, 1040, 1309, 1309, 1664, 3238, 3238, 3288
PG[c]	89.65	274, 322, 643, 912, 1033, 1124, 1148, 1469, 2133, 3098, 3198, 3370
intermediates		
cis − BPY	−1.58	196, 238, 516, 574, 746, 834, 902, 977, 1157, 1272, 1397, 1551, 3074, 3180, 3232
BAL	−90.87	158, 264, 357, 433, 722, 766, 878, 924, 1083, 1260, 1360, 1871, 3070, 3147, 3169
trans − BPY	−12.53	159, 257, 384, 702, 727, 882, 910, 943, 1237, 1255, 1351, 1549, 3094, 3180, 3228
CPB	16.46	205, 269, 482, 513, 683, 721, 820, 860, 929, 982, 1255, 1707, 3153, 3230, 3292
transition states		
TS1	90.01	158, 404, 414, 505, 598, 713, 742, 930, 1096, 1281, 1911, 2140, 3162, 3378, 815i
TS2	50.56	165, 302, 348, 470, 604, 694, 806, 930, 1087, 1312, 1797, 2629, 3221, 3298, 608i
TS3	53.55	179, 258, 344, 480, 561, 668, 790, 932, 1134, 1295, 1764, 2651, 3198, 3283, 632i
TS4	24.58	254, 314, 534, 629, 676, 761, 818, 1056, 1079, 1280, 1675, 3159, 3190, 3338, 213i
TS5	22.96	160, 280, 727, 848, 918, 923, 1006, 1027, 1070, 1160, 1554, 3186, 3235, 3278, 278i
TSr	70.50	177, 268, 505, 563, 746, 795, 813, 950, 1036, 1293, 1721, 2869, 3144, 3288, 448i

[a] See Figure 3 for the ionic structures corresponding to abbreviations. The calculated absolute energy and zero-point energy of PGB are −2689.860 371 and 0.044 10 hartrees, respectively. [b] Energy at the zero point referred to that of PGB. [c] Energy of Br neutral is included in the potential energy.

Table 1, which have not been scaled since the appropriate scaling factor for this level is not known even though that of 0.9614 was recommended for the B3LYP/6-31G* level.[35] The zero-point correction has been made for the potential energies of all the structures. Then, the energies at the zero points of these structures referred to that of PGB have been calculated. These are listed in Table 1 also. A schematic potential energy diagram pertinent to the dissociation of PGB near the threshold is shown in Figure 3.

The immediate precursor to the dissociation products CP + Br$^{\bullet}$ is obviously cyclopropenyl bromide ion (CPB), which was found to be formed by isomerization of the *trans*-1-bromo-1-propen-3-ylidene ion (CHCH═CHBr$^{\bullet+}$, *trans*-BPY), as shown in Figure 3. No direct pathway from PGB to *trans*-BPY could be found. On the other hand, isomerization of PGB to *cis*-BPY was found to occur with the critical energy comparable to that of the propargyl ion channel (reaction 2b). Two pathways for cis-to-trans isomerization of BPY were found; the direct isomerization and the two-step isomerization via the bromoallene ion (CH_2═C═CHBr$^{\bullet+}$, BAL). The latter is energetically more favorable than the former and is likely to be the major pathway, as will be shown later.

The dissociation step CPB → CP + Br$^{\bullet}$ has the reverse barrier of 33 kJ mol^{-1} (=0.34 eV) even though it is a bond cleavage

reaction. The fact that the cyclopropenium ion (CP) has the aromatic stability is responsible for the presence of the reverse barrier. Presence of a reverse barrier in the bond cleavage reaction has been reported for reactions involving aromatically stabilized products such as cyclopropene$^{\bullet+}$ → CP + H$^{\bullet}$,[13] methylcyclopropene$^{\bullet+}$ → methylcyclopropenium^{+} + H$^{\bullet}$,[14] cycloheptatriene$^{\bullet+}$ → tropylium^{+} + H$^{\bullet}$,[10] and ethylcycloheptriene$^{\bullet+}$ → tropylium^{+} + $C_2H_5^{\bullet}$.[9] Presence of the reverse barrier in the dissociation step, in turn, is responsible for the release of large energy into the relative translation of the products, as observed experimentally. We do not attempt a quantitative explanation for the experimental KERD here. A dynamical study involving classical trajectory calculation[6] would be needed for such an investigation.

RRKM Calculations. In the PEPICO study of Tsai et al.,[27] both CP and PG were observed with comparable intensities in the dissociation of PGB at the threshold. Hence, it was suggested that the critical energies for the two channels are nearly the same. These two critical energies are nearly the same in the quantum chemical calculations made in this work also. This is in agreement with the PEPICO result even though the critical energy (90 kJ mol^{-1} = 0.93 eV) calculated here is larger than that (0.52 eV) estimated from the experimental ionization and appearance energies reported in the above work.

To investigate the reactions in details, the rate-energy dependences have been calculated using the RRKM formalism[36] with the quantum chemical energy and structure data.

$$k(E) = \sigma \frac{W^{\ddagger}(E - E_0)}{h\rho(E)} \tag{3}$$

Here, E and E_0 are the parent ion internal energy and the critical energy for dissociation, respectively. $W^{\ddagger}$ is the sum of states at the TS. ρ is the density of states of the parent and σ is the reaction path degeneracy. The rate constants for all the steps involved in reaction 2a, both forward and backward, can be calculated straightforwardly using the information in Table 1. Uncertainty appears in the calculation of the rate constant for reaction 2b because the transition state cannot be identified. It is usual in such a loose transition state case to adjust the TS vibrational frequencies using the 1000 K activation entropy ($\Delta S^{\ddagger}$) as the guideline for the looseness.[37] The C−Br stretching vibration at 621 cm^{-1} was taken as the reaction coordinate. The rate-energy relation for this reaction was calculated using a $\Delta S^{\ddagger}$ of 29 J mol^{-1} K^{-1} (=7.0 cal mol^{-1} K^{-1}), which is a reasonable value for a reaction occurring via a loose transition state. The result is shown in Figure 4. The rate constant at the threshold is 2×10^8 s^{-1} in this case. It is well-known that the rate constant decreases as $\Delta S^{\ddagger}$ is reduced. When the rate was calculated with a $\Delta S^{\ddagger}$ of 13 J mol^{-1} K^{-1}, which can no longer be considered as a loose transition state case, the threshold rate constant of 4×10^7 s^{-1} was obtained. The rate-energy dependence for PGB → *cis*-BPY is shown in Figure 4 also. The rate constant at the threshold is 3×10^7 s^{-1} in this case. At the same threshold energy, the rate constants for the remaining steps, *cis*-BPY → CP + Br$^{\bullet}$, were found to be larger than the first step. Namely, the isomerization PGB → *cis*-BPY is the rate-determining step for the production of CP at the threshold. Then, the total dissociation rate constant of PGB is on the order of 10^8 s^{-1} at the threshold. This is in agreement with the observation of Tsai et al.[27] that the dissociation rate constant of PGB was larger than 10^7 s^{-1} near the threshold. On the other hand, the observation of MID on a much longer time scale (28 μs) cannot be explained by the conventional RRKM calculation on the potential energy surface obtained quantum chemically.

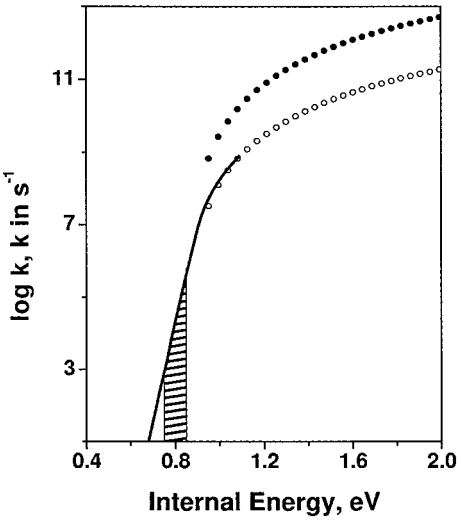

Figure 4. RRKM rate-energy relations for PGB → *cis*-BPY (○) and PGB → PG + Br$^{\bullet}$ (●). The rate-energy relation for the former corrected for the quantum mechanical tunneling is shown as the solid line (—). The shaded region corresponds to the internal energy range contributing to more than 95% of the dissociation via tunneling. See text for details of calculations.

It is well-known that the dissociation occurring slower than the threshold RRKM rate is often associated with the quantum mechanical tunneling. It is all the more plausible in this case because the H-atom transfer is involved in the rate-determining step, PGB → *cis*-BPY. The tunneling-corrected RRKM rate expression was reported by Miller.[15]

$$k_{\text{tun}}(E) = \sigma \frac{\int_0^E \kappa(\epsilon)\rho^{\ddagger}(E - \epsilon)\, \mathrm{d}\epsilon}{h\rho(E)} \tag{4}$$

Here, $\rho^{\ddagger}$ is the density of states at TS, ϵ is the energy in the one-dimensional reaction coordinate as measured from the zero-point energy of the reactant, and κ is the tunneling probability. The tunneling probability can be calculated by treating the barrier along the reaction coordinate as the Eckart potential.[38] The barrier heights and the imaginary frequency related to the barrier obtained by quantum chemical calculations can be used in the construction of the Eckart potential. The resulting rate-energy dependence for the isomerization PGB → *cis*-BPY is shown in Figure 4. Since the lifetime (τ) of the metastable PGB detected in this work is 28 ± 2 μs, it is likely that the observed MID is the result of quantum mechanical tunneling occurring below the threshold. Using the calculated rate-energy curve and the lifetime data, the internal energy distribution of PGB undergoing MID can be estimated from the random lifetime relation:[36] $P(E) \propto k(E) \exp[-k(E)\tau]$. The shaded region in Figure 4 corresponds to the internal energy range contributing to more than 95% of the distribution, which has the width of 0.1 eV. The average internal energy of PGB undergoing isomerization and subsequent dissociation is 0.80 eV, which is 0.13 eV below the RRKM reaction threshold. The average isomerization rate constant corresponding to this internal energy is 1.9×10^4 s^{-1}. This is also the average overall dissociation rate constant because PGB → *cis*-BPY is the rate-determining step in the production of CP.

It has been argued so far that the dissociation of PGB to CP can occur on a tens of microsecond time scale through quantum mechanical tunneling even though the reaction would be completed well within 1 μs at the classical threshold energy. One final question that remains to be answered is why then the

same slow decomposition could not be observed in the previous experiment with the PEPICO technique, which is capable of determining the rate constant in the range 10^4-10^5 s^{-1}. The answer seems to lie in the fact that the energy difference between the classical threshold and the level at which tunneling occurs is very small (0.13 eV) and that the parent ion internal energy in PEPICO is not sharp but has a distribution due to the thermal energy. Namely, it is not possible in PEPICO to select only those metastable ions with internal energy just below the threshold. Molecular ions with internal energy at or just above the threshold tends to be selected simultaneously. The latter ions, which dissociate much more efficiently, will dominate the PEPICO peak profile. The slow dissociation may also occur but will form an insignificant tail in the profile. In the present MID experiment, all the molecular ions generated with the internal energy at or above the classical threshold dissociate inside the ion source. Physical separation of the ion source and the dissociation region allows observation of only those dissociation events occurring after a definite time delay.

Dissociation of the Bromoallene Molecular Ion. It was mentioned earlier that the cis-to-trans isomerization of BPY can occur via two different pathways: the direct isomerization and the two-step isomerization via the bromoallene (BAL) ion.

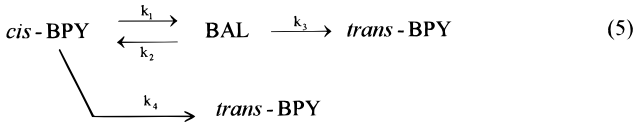

(5)

The solution of the rate equation for reactions similar to reaction 5 has been reported already,[39] and the fraction of *trans*-BPY generated in each channel can be calculated once the rate constants are known. We calculated the rate constants by the RRKM formula using the data in Table 1 at the internal energy of 0.80 eV referred to PGB, namely for *cis*-BPY generated by the quantum mechanical tunneling. These were 6.2×10^{10}, 6.7×10^7, 4.3×10^7, and 5.3×10^8 s^{-1} for k_1, k_2, k_3, and k_4, respectively. With these rate constants, the two-step channel was found to be dominant, generating 98% of the *trans*-BPY ion. If the mechanistic pathway for the dissociation of PGB determined by the quantum chemical calculation is qualitatively correct and BAL is an intermediate, its MID-MIKE profile is expected to appear as dish-topped also because of the large kinetic energy release in the dissociation step. In this regard, we synthesized the bromoallene molecule and recorded the MID-MIKE profile of the BAL ion. The MID-MIKE profile thus obtained and the KERD evaluated therefrom also were essentially identical to those in Figure 1, confirming our expectation. This indicates that the PES determined by the quantum chemical calculations provide a good qualitative picture for the mechanistic pathway for the dissociation of the PGB ion. As a matter of fact, the near identity of the two experimental KERDs is a little annoying. Calculation of the rate constant for the dissociation of BAL using data in Table 1 in the same manner as for PGB showed that the reaction occurs just at or slightly below (0.04 eV) its threshold (TS3). Then, the ions arriving at the final transition state, TS5, from BAL would have an internal energy smaller (by about 0.3 eV) than those from PGB, leading to less kinetic energy release. It is to be mentioned, however, that such an internal energy may be distributed randomly in all the internal degrees of freedom according to the RRKM picture and only a fraction of it may appear as the kinetic energy release. More importantly, one would not expect that quantum chemical calculations provide a quantitatively accurate description of the mechanistic pathway. One interesting possibility is, then, that the isomerization barriers for PGB → BAL are low and the two structures are in equilibrium prior to dissociation. Namely, when the heights of TS1 and TS2 are sufficiently lower than that of TS3, KERDs in the dissociation of $C_3H_3Br^{\bullet+}$ produced from the propargyl bromide and bromoallene neutrals can become essentially the same. As a partial check of such a possibility, we obtained the CID-MIKE spectra of $C_3H_3Br^{\bullet+}$ generated from the two precursor neutrals, which are shown in Figure 5. $C_3H_3^+$ is the dominant product in the collision-induced dissociation of $C_3H_3Br^{\bullet+}$ ions, and the two spectra look similar in this sense. Other than that, the two spectra display a noticeable difference in the intensities of the minor but important fragment ions such as $C_3H_3Br^{2+}$, CBr^+, $CHBr^{\bullet+}$, CH_2Br^+, and $C_2HBr^{\bullet+}$. It is well-known that a distinct difference in the CID spectral patterns of ions with the same chemical formula is an indication that the ions have different molecular structures or that they are the mixtures with different isomeric compositions.[40] Namely, the PGB and BAL structures do not seem to freely interconvert to each other. This is in agreement with the qualitative mechanistic picture presented by the potential energy surface obtained by the quantum chemical calculations and hence supports the mechanistic interpretation for the dissociation of PGB proposed in this work.

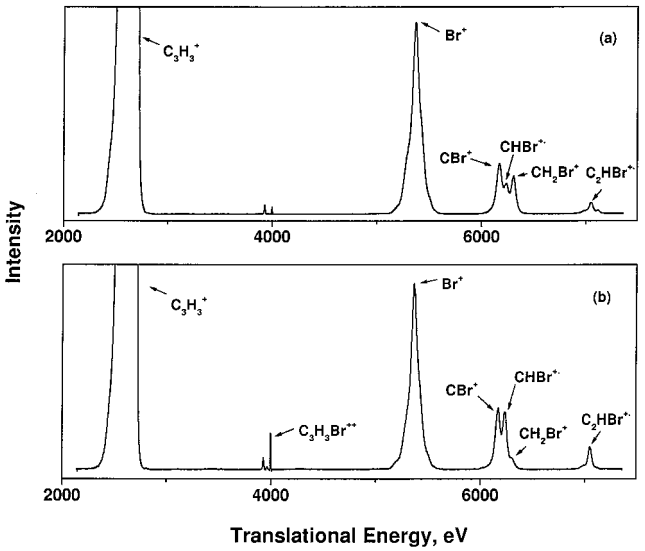

Figure 5. CID-MIKE spectra of $C_3H_3Br^{\bullet+}$ generated from (a) propargyl bromide and (b) bromoallene neutrals.

5. Concluding Remarks

Observation of large kinetic energy releases in the unimolecular dissociation of $C_3H_3Br^{\bullet+}$ has shown that the product $C_3H_3^+$ ion has the cyclopropenium structure rather than the propargyl one. The potential energy surface along a plausible mechanistic pathway of this reaction could be obtained on the B3LYP/6-311G** density functional theory level of the quantum chemical calculation. The RRKM rate calculation on this surface with and without the tunneling correction has shown that the isomerization of the propargyl bromide ion to the *cis*-1-bromo-1-propen-3-ylidene structure is the rate-determining step and that the observed reaction occurs via quantum mechanical tunneling at ~0.1 eV below the threshold. The reaction changes abruptly at and above the threshold and the simple bond cleavage to the propargyl structure becomes important. Since the corresponding change in the internal energy is very small, the phenomenon cannot be easily detected by the usual ion kinetic techniques such as PEPICO. Definite physical and

temporal separations of the ionization and dissociation events in the metastable ion decomposition technique have been found to be especially useful in the present study.

One final remark concerns the origin of the substantial kinetic energy release in the present reaction. It is certain that a substantial fraction of the final reverse barrier between TS5 and CP + Br$^{\bullet}$ would appear as the kinetic energy release. The RRKM rate calculation for the passage of TS4 and TS5 (not presented) shows, however, that the process occurs within a picosecond for ions that have passed the barrier at TS3. This may not be a sufficient time for a complete intramolecular vibrational relaxation. A nonstatistical partitioning of the excess energy near the final saddle point (TS5) may result in a larger kinetic energy release than statistically expected. A more rigorous dynamical study, such as those employing the classical trajectory method, would be needed to probe this interesting situation.

Acknowledgment. This work was supported financially by CRI, the Ministry of Science and Engineering, Republic of Korea.

References and Notes

(1) Hase, W. L.; Wolf, R. J. In *Potential Energy Surfaces and Dynamics Calculations*; Truhlar, D. G., Ed.; Plenum: New York, 1981; p 37.

(2) Kato, S.; Morokuma, K. *J. Chem. Phys.* **1980**, *73*, 3900. Lynch, G. C.; Truhlar, D. G.; Brown, F. B.; Zhao, J.-g. *J. Phys. Chem.* **1995**, *99*, 207. Benito, R. M.; Santamaria, J. *J. Phys. Chem.* **1988**, *92*, 5028.

(3) Rice, B. M.; Adams, G. F.; Page, M.; Thompson, D. L. *J. Phys. Chem.* **1995**, *99*, 5016. Abrash, S. A.; Zehner, R. W.; Mains, G. J.; Raff, L. M. *J. Phys. Chem.* **1995**, *99*, 2959. Raff, L. M.; Graham, R. W. *J. Phys. Chem.* **1988**, *92*, 5111. Chen, W.; Hase, W. L.; Schlegel, H. B. *Chem. Phys. Lett.* **1994**, *228*, 436.

(4) Ma, N. L.; Radom, L.; Collins, M. A. *J. Chem. Phys.* **1992**, *96*, 1093.

(5) Rhee, Y. M.; Lee, T. G.; Park, S. C.; Kim, M. S. *J. Chem. Phys.* **1997**, *106*, 1003.

(6) Lee, T. G.; Park, S. C.; Kim, M. S. *J. Chem. Phys.* **1996**, *104*, 4517. Helgaker, T.; Uggerud, E.; Jensen, H. J. A. *Chem. Phys. Lett.* **1990**, *173*, 145. Uggerud, E.; Helgaker, T. *J. Am. Chem. Soc.* **1992**, *114*, 4265.

(7) Morrow, J. C.; Baer, T. *J. Phys. Chem.* **1988**, *92*, 6567. Schroder, D.; Sulzle, D.; Dutuit, O.; Baer, T.; Schwarz, H. *J. Am. Chem. Soc.* **1994**, *116*, 6395. Mayer, P. M.; Baer, T. *J. Phys. Chem.* **1996**, *100*, 14949.

(8) Booze, J. A.; Weitzel, K.-M.; Baer, T. *J. Chem. Phys*. **1991**, *94*, 3649. Mazyar, O. A.; Mayer, P. M.; Baer, T. *Int. J. Mass Spectrom. Ion Processes* **1997**, *167/168*, 389. Keister, J. W.; Baer, T.; Thissen, R.; Alcaraz, C.; Dutuit, O.; Audier, H.; Troude, V. *J. Phys. Chem. A* **1998**, *102*, 1090. Mazyar, O. A.; Baer, T. *J. Phys. Chem. A* **1998**, *102*, 1682.

(9) Hwang, W. G.; Moon, J. H.; Choe, J. C.; Kim, M. S. *J. Phys. Chem. A* **1998**, *102*, 7512.

(10) Lifshitz, C.; Gotkis, Y.; Ioffe, A.; Laskin, J.; Shaik, S. *Int. J. Mass Spectrom. Ion Processes* **1993**, *125*, R7.

(11) Chalk, A. J.; Radom, L. *J. Am. Chem. Soc.* **1998**, *120*, 8430.

(12) Klippenstein, S. J. *Int. J. Mass Spectrom. Ion Processes* **1997**, *167/168*, 235.

(13) Frenking, G.; Schwarz, H. *Int. J. Mass Spectrom. Ion Phys.* **1983**, *52*, 131.

(14) Hrouda, V.; Cársky, P.; Ingr, M.; Chval, Z.; Sastry., G. N.; Bally, T. *J. Phys. Chem. A* **1998**, *102*, 9297.

(15) Miller, W. H. *J. Am. Chem. Soc.* **1979**, *101*, 6810.

(16) Lorquet, J. C. *Mass Spectrom. Rev.* **1994**, *13*, 233.

(17) Baer, T. *Adv. Chem. Phys.* **1986**, *64*, 111.

(18) Bowers, M. T.; Marshall, A. G.; McLafferty, F. W. *J. Phys. Chem.* **1996**, *100*, 12897. Hanratty, M. A.; Beauchamp, J. L.; Illies, A. J.; Koppen, P.; Bowers, M. T. *J. Am. Chem. Soc.* **1988**, *110*, 1.

(19) Choe, J. C.; Kim, M. S. *Int. J. Mass Spectrom. Ion Processes* **1991**, *107*, 103.

(20) Cho, Y. S.; Kim, M. S.; Choe, J. C. *Int. J. Mass Spectrom. Ion Processes* **1995**, *145*, 187.

(21) Lifshitz, C.; Levin, I.; Kababia, S.; Dunbar, R. C. *J. Phys. Chem.* **1991**, *95*, 1667.

(22) Szulejko, J. E.; Mendez Amaya, A.; Morgan, R. P.; Brenton A. G.; Beynon, J. H. *Proc. R. Soc. London, Ser. A* **1980**, *373*, 1.

(23) Terwilliger, D. T.; Beynon, J. H.; Cooks, R. G. *Int. J. Mass Spectrom. Ion Phys.* **1975**, *16*, 225.

(24) Rumpf, B. A.; Derrick, P. J. *Int. J. Mass Spectrom. Ion Processes* **1988**, *82*, 239.

(25) Yeh, I. C.; Kim, M. S. *Rapid Commun. Mass Spectrom*. **1992**, *6*, 115, 293.

(26) Baer, T.; Werner, A. S.; Tsai, B. P. *J. Chem. Phys.* **1975**, *62*, 2497.

(27) Tsai, B. P.; Werner, A. S.; Baer, T. *J. Chem. Phys.* **1975**, *63*, 4384.

(28) Krailler, R. E.; Russell, D. H. *Int. J. Mass Spectrom. Ion Processes* **1985**, *66*, 339.

(29) Holmes, J. L.; Lossing, F. P. *Can. J. Chem.* **1979**, *57*, 249.

(30) Burgers, P. C.; Holmes, J. L.; Mommers, A. A.; Szulejko, J. E. *J. Am. Chem. Soc.* **1984**, *106*, 521.

(31) Ausloos, P. J.; Lias, S. G. *J. Am. Chem. Soc.* **1981**, *103*, 6505.

(32) NIST Standard Reference Database 69, Nov 1998: *NIST chemistry WebBook*.

(33) Jacobs, T. L.; Brill, W. F. *J. Am. Chem. Soc.* **1953**, *75*, 1314.

(34) Frisch, M. J.; Trucks, G. W.; Schlegel, H. B.; Gill, P. M. W.; Johnson, B. G.; Robb, M. A.; Cheeseman, J. R.; Keith, T.; Petersson, G. A.; Montgomery, J. A.; Raghavachari, K.; Cioslowski, J.; Stefanov, B. B.; Nanayakkara, A.; Challacombe, M.; Peng, C. Y.; Ayala, P. Y.; Chen, W.; Wong, M. W.; Andres, J. L.; Replogle, E. S.; Gomperts, R.; Martin, R. L.; Fox, D. J.; Binkley, J. S.; Defrees, D. J.; Baker, J.; Stewart, J. P.; Head-Gordon, M.; Gonzalez, C.; Pople, J. A. *GAUSSIAN 94*, revision E.2; Gaussian, Inc.: Pittsburgh, PA, 1995.

(35) Scott, A. P.; Radom, L. *J. Phys. Chem.* **1996**, *100*, 16502.

(36) Robinson, P. J.; Holbrook, K. A. *Unimolecular Reactions*; Wiley: New York, 1972.

(37) Lifshitz, C. *Mass Spectrom. Rev.* **1982**, 1, 309; *Adv. Mass Spectrom.* **1989**, *11*, 713.

(38) Eckart, C. *Phys. Rev.* **1930**, *35*, 1303.

(39) Oh, S. T.; Choe, J. C.; Kim, M. S. *J. Phys. Chem.* **1996**, *100*, 13367.

(40) Levsen, K. *Fundamental Aspects of Organic Mass Spectrometry*; Verlag Chimie: Weinheim, 1978.